Electronic Supplementary Material (ESI) for Journal of Materials Chemistry A.

Electronic Supplementary Information (ESI)

Hierarchical MnCo-Layered Double Hydroxides@Ni$(OH)_2$ Core-Shell Heterostructures as Advanced Electrode for Supercapacitors

Shude Liu[a], Iman Shackery[a], Umakant Patil[a], Su Chan Lee[a,b], Byeongho Park[a], Hye bin An[a], Kyung Yoon Chung[a,b], Seong Chan Jun[a,*]

[a]Nano-Electro Mechanical Device Laboratory, School of Mechanical Engineering, Yonsei University, Seoul 120-749, South Korea.

[b]Center for Energy Convergence Research, Korea Institute of Science and Technology, Hwarang-ro 14-gil 5, Seongbuk-gu, Seoul 136-791, Republic of Korea

[*]*Corresponding author:*

E-mail: scj@yonsei.ac.kr *(Seong Chan Jun)*

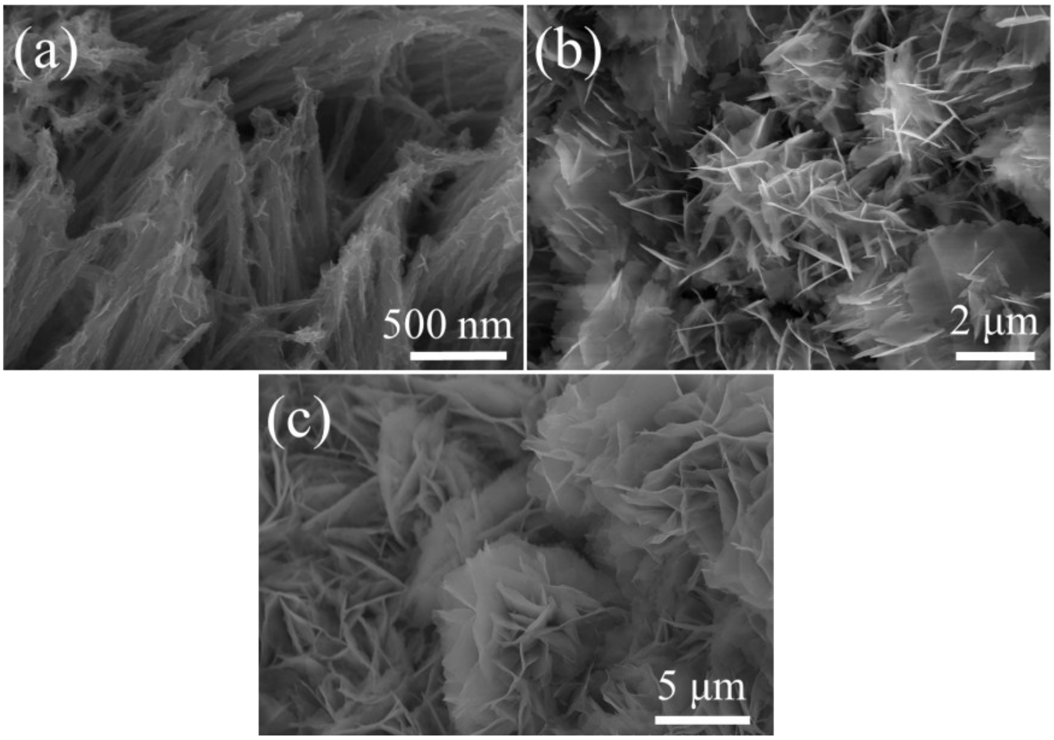

Figure S1. SEM images of MnCo-LDH@$Ni(OH)_2$ core–shell heterostructures obtained with various $Ni(OH)_2$ deposition time: (a) 4 h, (b) 12 h, (c) 20 h, respectively.

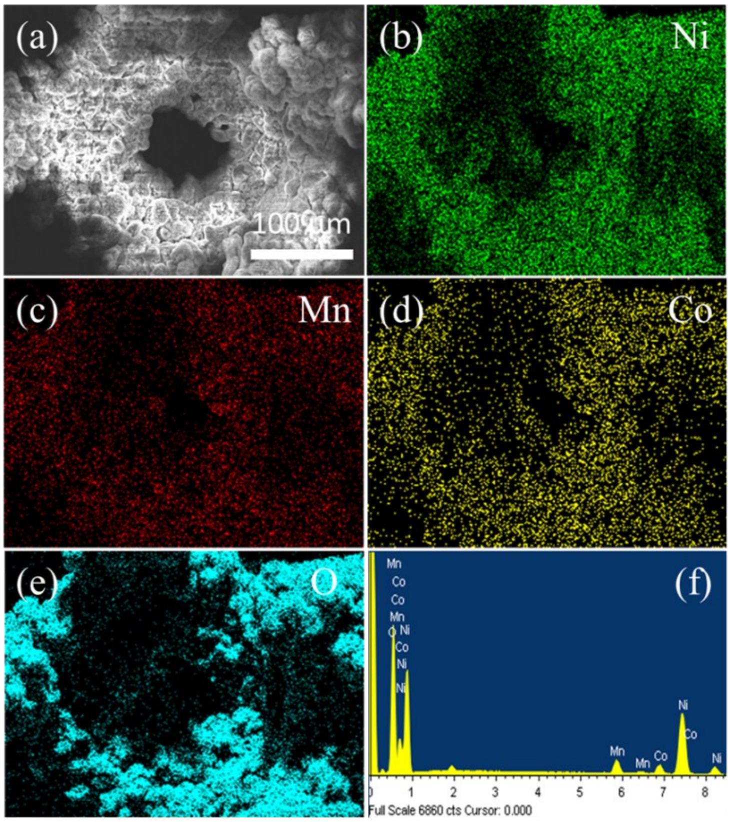

Figure S2 (a) SEM image with corresponding elemental mapping images of (b) Ni, (c) Mn, (d) Co, and (e) O. (f) EDS spectrum of the MnCo-LDH@Ni$(OH)_2$-12 h core–shell heterostructures.

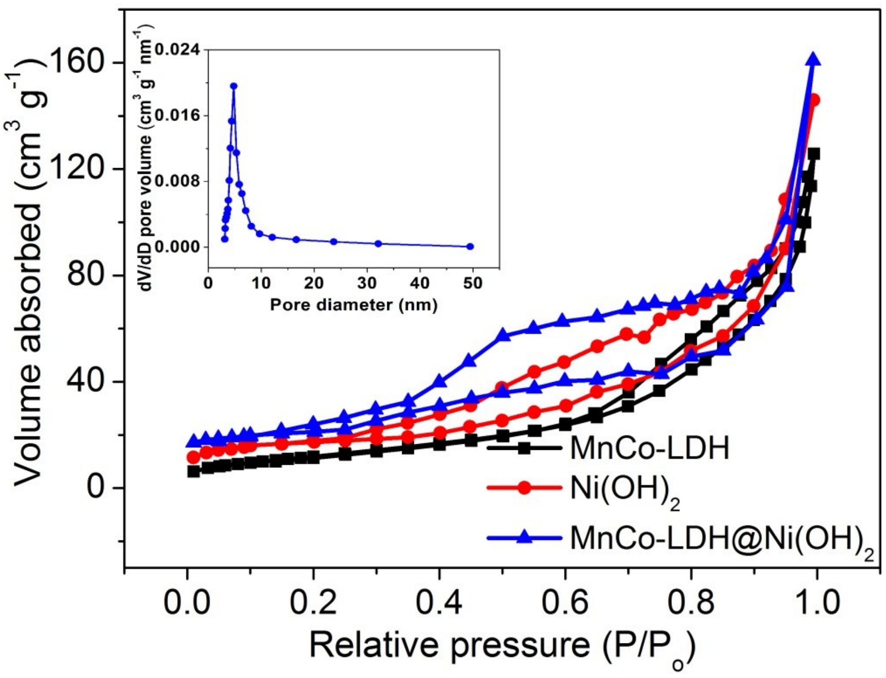

Figure S3 (a) Nitrogen adsorption/desorption isotherms of MnCo-LDH, $Ni(OH)_2$ and MnCo-LDH@$Ni(OH)_2$-12 h samples (Inset is the pore-size distribution of MnCo-LDH@$Ni(OH)_2$-12 h).

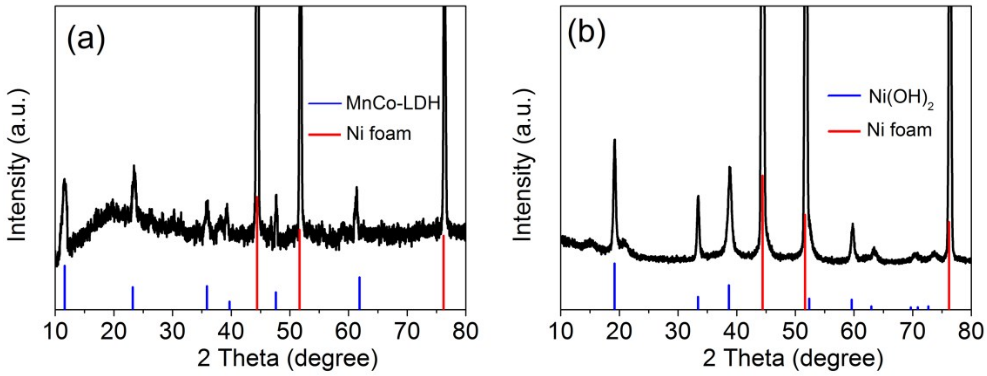

Figure S4 XRD patterns of (a) MnCo-LDH and (b) $Ni(OH)_2$ supported on Ni foam.

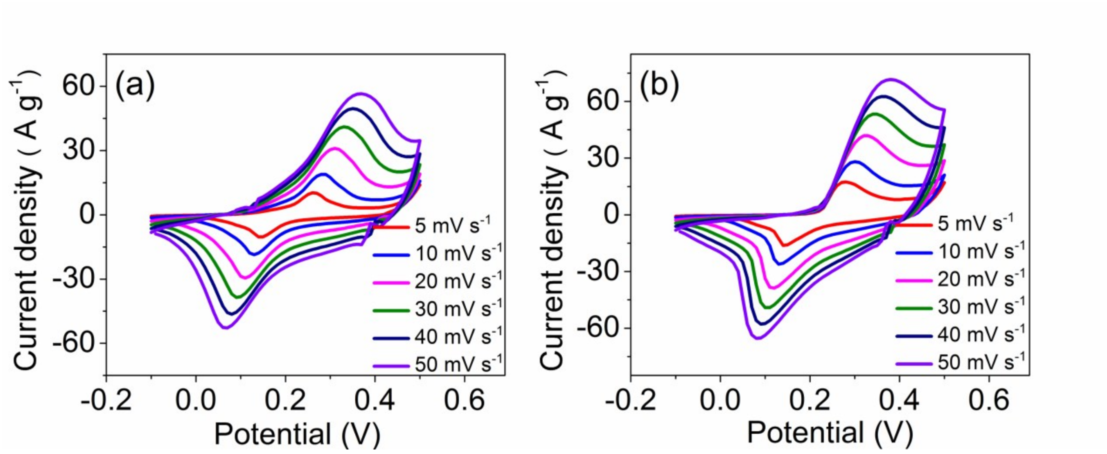

Figure S5 CV curves of (a) MnCo-LDH nanowire and (b) $Ni(OH)_2$ nanosheet electrodes at different scan rates.

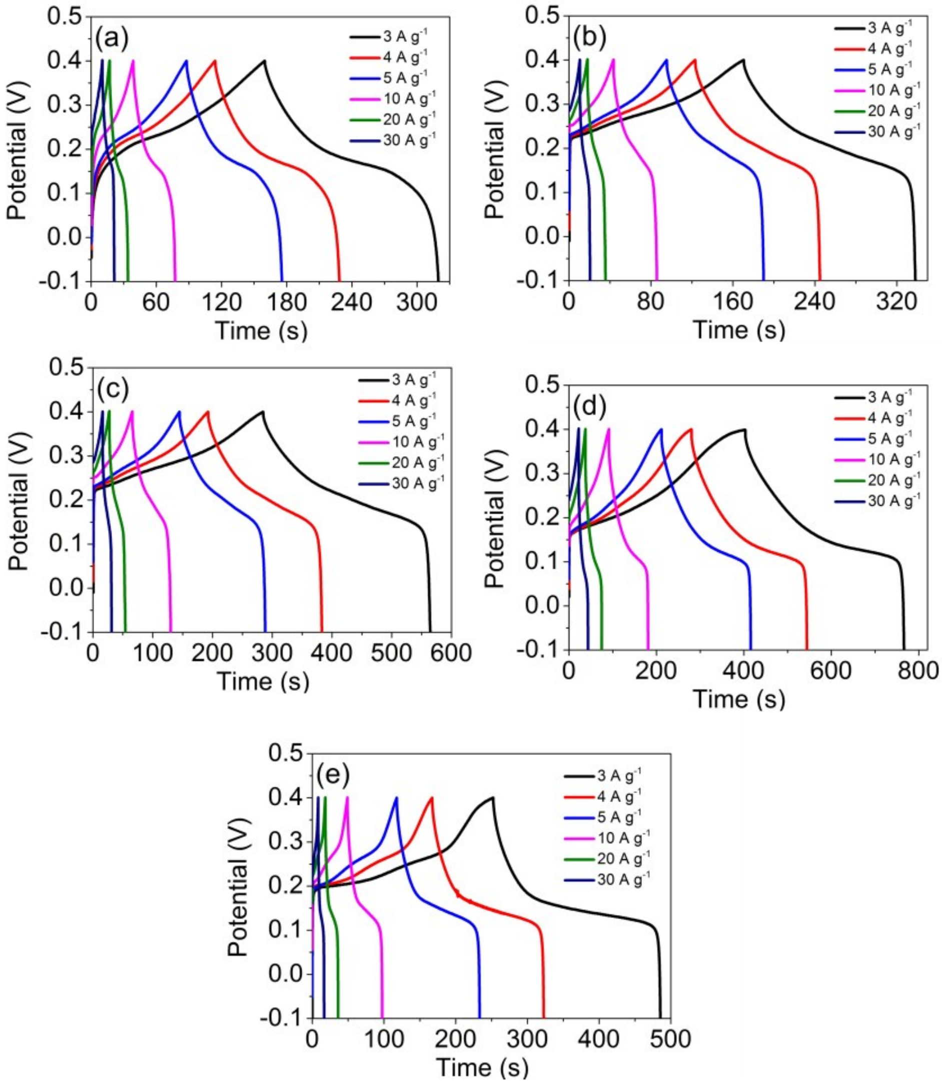

Figure S6 GCD curves of (a) MnCo-LDH, (b) $Ni(OH)_2$, and (c-e) MnCo-LDH@$Ni(OH)_2$ ($Ni(OH)_2$ deposition time: 4, 12, and 20 h, respectively) at various current densities.

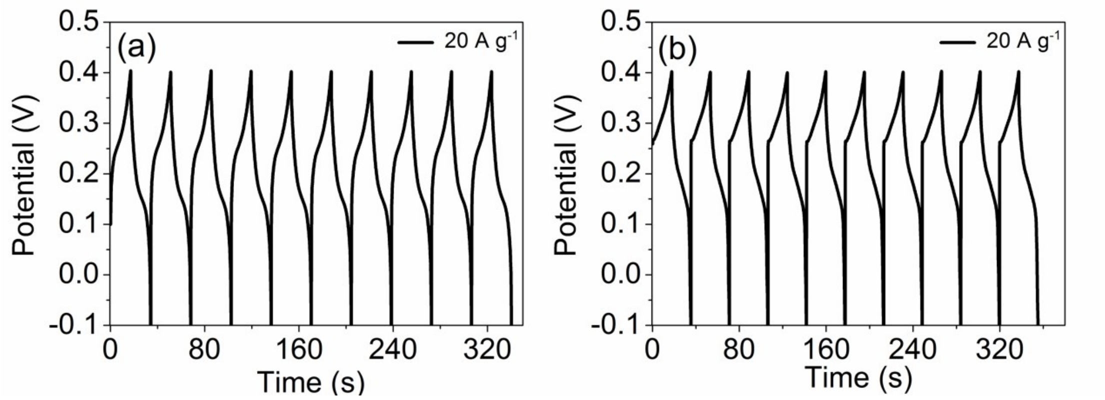

Figure S7 GCD curves of the first 10 cycles for (a) MnCo-LDH and (b) $Ni(OH)_2$ electrodes in the potential window of −0.1 to 0.4 V at a current density of 20 A g^{-1}.

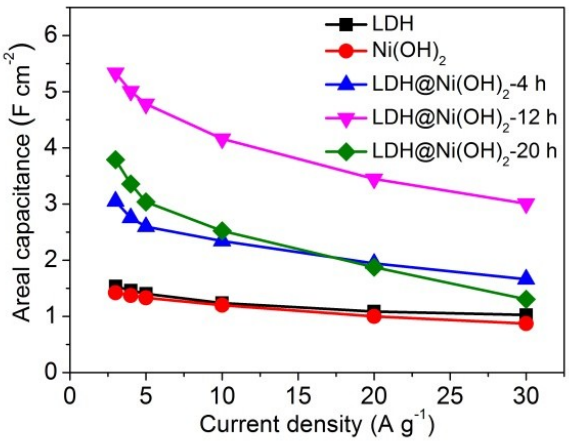

Figure S8 Areal capacitance values of the prepared electrodes conducted at different current densities

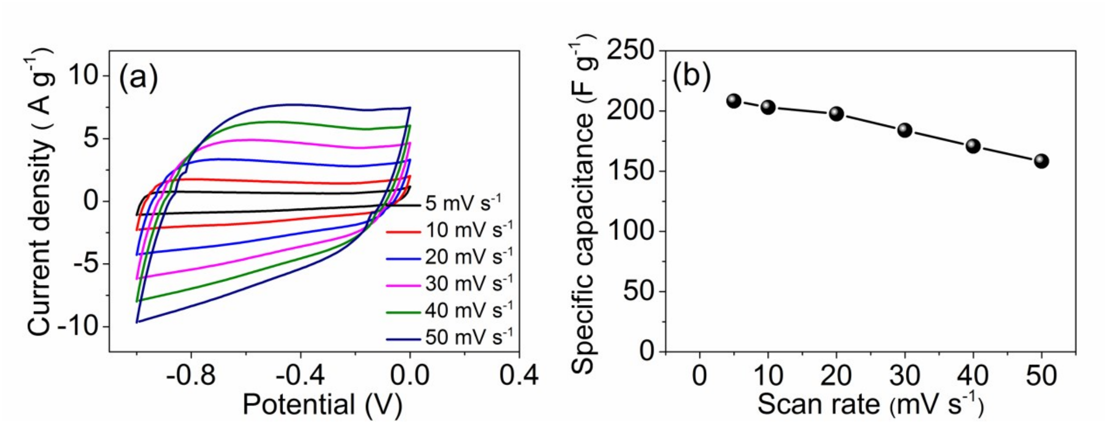

Figure S9 (a) CV curves and (b) the corresponding specific capacitances of activated carbon recorded at different scan rates.

Table S1 Electrochemical performances comparison of MnCo-LDH@$Ni(OH)_2$ heterostructures with previous reports on LDH-based hybrid electrodes.

Materials	Specific capacitance (current destiny/scan rate)	Capacitance retention (cycles)	Ref
Graphene/NiAl-LDH nanoparticles	213.57 F g^{-1} (1 A g^{-1})	≈100% (1000)	S1
GNS/NiAl-LDH nanoplatelets	781.5 F g^{-1} (5 mV s^{-1})	122.56% (200)	S2
CoAl-LDH nanosheets/GNS	484.8 F g^{-1} (2 A g^{-1})	/	S3
CoAl-LDH nanoplatelets/MnO_2 nanoparticles	1088 F g^{-1} (1 A g^{-1})	≈100% (1000)	S4
$Co_{0.41}Ni_{0.59}$-LDH microparticles	1809 F g^{-1} (1 A g^{-1})	/	S5
platelet-like NiAl-LDH particles	701 F g^{-1} (10 mA cm^{-2})	94% (400)	S6
NiTi-LDH thin films	10.37 F cm^{-2} (5 mA cm^{-2})	86% (1000)	S7
GS/NiCo-LDH nanoflakes	1980.7 F g^{-1} (1 A g^{-1})	97.1% (1500)	S8
CoAl-LDH nanosheets/GO	772 F g^{-1} (1 A g^{-1})	73% (10000)	S9
CoAl-LDH flakes	342.4 F g^{-1} (2 A g^{-1})	/	S10
NiCoAl-LDH nanosheets /CNT	1188 F g^{-1} (1 A g^{-1})	90%(1000)	S11
CoAl-LDH nanosheets/GO	1031 F g^{-1} (1 A g^{-1})	≈100% (6000)	S12
CoAl-LDH nanosheets /GO	880 F g^{-1} (5 mV s^{-1})	≈100% (2000)	S13
CoAl-LDH nanosheets/CNT	884 F g^{-1} (0.86 A g^{-1})	88% (2000)	S14

a-GNS/NiAl-LDH nanoflakes	790 A g^{-1} (10 A g^{-1})	99.2% (500)	S15
MnCo-LDH@$Ni(OH)_2$	2320 A g^{-1} (3 A g^{-1})	90.9% (5000)	Present work

S1. Z. Wang, X. Zhang, J. Wang, L. Zou, Z. Liu and Z. Hao, *Journal of colloid and interface science*, 2013, **396**, 251-257.

S2. Z. Gao, J. Wang, Z. Li, W. Yang, B. Wang, M. Hou, Y. He, Q. Liu, T. Mann and P. Yang, *Chemistry of Materials*, 2011, **23**, 3509-3516.

S3. S. Huang, G.-N. Zhu, C. Zhang, W. W. Tjiu, Y.-Y. Xia and T. Liu, *ACS applied materials & interfaces*, 2012, **4**, 2242-2249.

S4. Z. P. Diao, Y. X. Zhang, X. D. Hao and Z. Q. Wen, *Ceramics International*, 2014, **40**, 2115-2120.

S5. H. ZA, Y. XIE and Y. WANG, *J Electrochimica Acta*, 2009, **54**, 2737-2741.

S6. J. Wang, Y. Song, Z. Li, Q. Liu, J. Zhou, X. Jing, M. Zhang and Z. Jiang, *Energy & Fuels*, 2010, **24**, 6463-6467.

S7. Y. H. Gu, Z. Y. Lu, Z. Chang, J. F. Liu, X. D. Lei, Y. P. Li and X. M. Sun, *J Mater Chem A*, 2013, **1**, 10655-10661.

S8. T. Yan, R. Li and Z. Li, *Materials Research Bulletin*, 2014, **51**, 97-104.

S9. J. Fang, M. Li, Q. Li, W. Zhang, Q. Shou, F. Liu, X. Zhang and J. Cheng, *Electrochimica Acta*, 2012, **85**, 248-255.

S10. Y. Ding, G. Gu and X.-H. Xia, *Journal of Solid State Electrochemistry*, 2008, **12**, 553-558.

S11. C. Yu, J. Yang, C. Zhao, X. Fan, G. Wang and J. Qiu, *Nanoscale*, 2014, **6**, 3097-3104.

S12. X. YiáDong, Z. JunáZhang, X. FengáPei and X. JiangáChen, *Chemical Communications*, 2011, **47**, 3556-3558.

S13. X. Dong, L. Wang, D. Wang, C. Li and J. Jin, *Langmuir*, 2011, **28**, 293-298.

S14. L. Yu, N. Shi, Q. Liu, J. Wang, B. Yang, B. Wang, H. Yan, Y. Sun and X. Jing, *Physical Chemistry Chemical Physics*, 2014, **16**, 17936-17942.

S15. N. Yulian, L. Ruiyi, L. Zaijun, F. Yinjun and L. Junkang, *Electrochimica Acta*, 2013, **94**, 360-366.